

---

# Segmentation of Soil Degradation Sites in Swiss Alpine Grasslands with Deep Learning

---

Maxim Samarin<sup>1,\*</sup>, Lauren Zweifel<sup>2,\*</sup>, Christine Alewell<sup>2</sup>, and Volker Roth<sup>1</sup>

<sup>1</sup>Department of Mathematics and Computer Science, <sup>2</sup>Department of Environmental Sciences  
University of Basel, Switzerland

{maxim.samarin, lauren.zweifel, christine.alewell, volker.roth}@unibas.ch

## Abstract

Soil degradation is an important environmental problem which affects the Alpine ecosystem and agriculture. Research results suggest that soil degradation in Swiss Alpine grasslands has increased in recent years and it is expected to increase further due to climate and land-use change. However, reliably quantifying the increase in spatial extent of soil degradation is a challenging task. Although methods like Object-based Image Analysis (OBIA) can provide precise detection of erosion sites, an efficient large scale investigation is not feasible due to the labour intensive nature and lack of transferability of the method. In this study, we overcome these limitations by adapting the fully convolutional neural network U-Net trained on high-quality training data provided by OBIA to enable efficient segmentation of erosion sites in high-resolution aerial images. We find that segmentation results of both methods, OBIA and U-Net, are generally in good agreement, but display method specific difference, with an overall precision of 73% and recall of 84%. Importantly, both methods indicate an increase in soil degradation for a case study region over a 16-year period of 167% and 201% for OBIA and U-Net, respectively. Furthermore, we show that the U-Net approach transfers well to new regions (within our study region) and data from subsequent years, even when trained on a comparably small training dataset. Thus the proposed approach enables large scale analysis in Swiss Alpine grasslands and provides a tool for reliable assessment of temporal changes in soil degradation.

## 1 Introduction

Soil degradation in Alpine grasslands is a major ecological threat which can affect substantial areas but is often difficult to assess from the ground, making a mapping and comprehensive understanding of these processes a challenging problem. Soil degradation or erosion phenomena often occur due to the steep topography, a pronounced exposure to wind, rain or snow, a particular geological composition or human influence. Recent studies on climate change suggest that for the Swiss Alps temperature increases, stronger and more frequent precipitation events, and altered snow dynamics have to be expected [1]. Additionally, with changing agricultural land use practice, soil erosion sites in Swiss Alpine grasslands are expected to increase in the future [12, 13]. It is therefore crucial to gain understanding of ongoing erosion processes to assess and adapt management practices.

---

\*Both authors contributed equally.

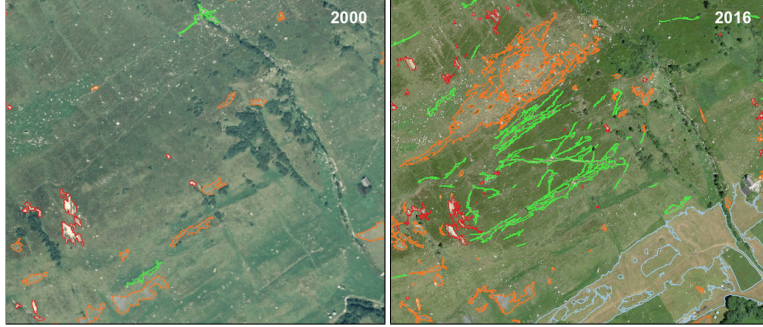


Figure 1: Increase of soil degradation sites in a case study region in the Swiss Alps. A section of about  $500 \text{ m} \times 500 \text{ m}$  in aerial images of the years 2000 and 2016 is displayed. Grassland, trees, rocks, and small buildings are visible as well as patches with disturbed vegetation or degraded soil. In the left image from 2000, three types of soil degradation sites are outlined in red, green, and orange (more information on the classes below). In comparison, the right image from 2016 exhibits more soil degradation sites. Overall, all four soil degradation classes increase over time. The segmentation outlines are obtained with the Object-based Image Analysis method (covered below) which employs Random Forests classification. The original section without class outlines is provided in fig. 2.

## 2 Methodology

In order to determine the temporal and spatial changes of soil erosion sites in the Alpine region, we make use of high-resolution aerial images on which erosion sites are visible (an example is shown on the left image of fig. 2). These *orthophotos* are corrected for terrain and camera specific distortions and contain the visual spectral bands (i.e. RGB) with a resolution of 0.5 m (before 2010) and 0.25 m (from 2010 on) provided by the Swiss Federal Office of Topography (Swisstopo) as the *Swissimage* product [15]. In addition, we use *digital elevation models* (DEM) which represent height information (pixel-wise) on a raster to derive a terrain's slope, curvature, and aspect. For this, the Swisstopo product *swissALTI3D* with a resolution of 2 m is used [16].

In this work, we focus on the Urseren Valley in the Swiss Alps (canton Uri, Switzerland) as a case study region (of about  $26 \text{ km}^2$ ) which is known to exhibit different erosion phenomena and for which aerial images for the years 2000, 2004, 2010, 2013, and 2016 are available. In accordance with [19], we distinguish between four erosion classes which will be briefly defined: **Shallow Landslide**, **Livestock Trails**, **Management Effects**, and **Sheet Erosion**.<sup>2</sup> Shallow landslides are characterised by their compact, almost vegetation free shape with clear boundaries and can be caused by heavy rain events or snow abrasion removing the topsoil layer. Livestock trails are elongated, narrow paths caused by movement of cattle and sheep. Management effects describe large compact areas which are due to agricultural use with heavy machinery. Finally, we also consider patches of sparse vegetation affected by sheet erosion (removal of soil particles by surface water runoff).

A state of the art approach for object detection tasks in the field of remote sensing is *Object-based Image Analysis* (OBIA) [2]. In a first step, the OBIA method segments the input image with a multi-resolution segmentation algorithm and then, in a second step, classifies the segments according to their spectral and spatial properties with classifiers like Support Vector Machines or Random Forests. OBIA is a semi-automated method capable of providing precise segmentations but requires domain expertise and manual adjustments which renders the application time consuming. In addition, the method is susceptible to small changes in the input images such as colour shifts due to different measurement devices or light conditions (see appendix fig. A2 for examples of colour variability). Therefore, the method needs to be applied to each input image separately which makes it difficult to use OBIA on a large scale.

In order to address these drawbacks and enable large scale analysis of soil degradation, we make use of the fully convolutional neural network architecture *U-Net* for semantic segmentation [14]. It is successfully used in biomedical imaging applications, e.g. [3, 4], and extensions to probabilistic frameworks were proposed [10]. U-Nets and similar approaches were used to address related remote

<sup>2</sup>The colours of the classes correspond to the colours of the respective class outlines in figures 1, 2, and A3 .

sensing tasks like segmentation of vegetation [5, 8], forest damage assessment [6], or building identification [7, 11, 17, 18] in satellite or aerial imagery. In our study, we extend the U-Net to allow for incorporating additional layers of information, such as the raster images for slope, curvature, and aspect by concatenating these as additional channels with the actual RGB input image. See appendix fig. A1 for a schematic illustration of the employed network. The ground truth segmentation is generated with the OBIA method applied to the aerial image of the case study site for the different years (following [19]). Training samples of the years 2000, 2004, 2010, and 2013 are extracted from the aerial images to form a total of 1292 training samples (see appendix fig. A2). A dedicated validation section (of about  $17 \text{ km}^2$ ) is excluded from training. Validation of the trained U-Net is then performed on the held-out validation section and the aerial image of 2016. In our experiments, a U-Net of depth three (i.e. two max-pooling steps) yielded the best results. The network was trained from scratch for 300 epochs with a batch size of 20 and a dropout rate of 0.1. Further, the Adam optimiser [9] with a learning rate of 0.001 was used.

### 3 Results and Discussion

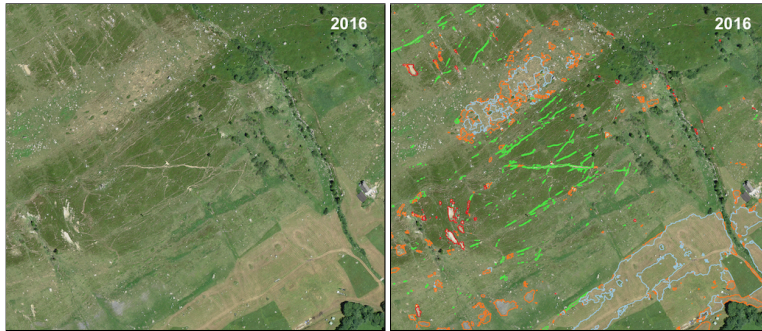


Figure 2: Segmentation results for the case study region obtained with a U-Net (with a threshold of 0.3). Again, a section of about  $500 \text{ m} \times 500 \text{ m}$  in the aerial image of 2016 is shown. On the left the input image is given and the segmentation outlines are shown on the right. The detected soil degradation sites exhibit good correspondence to the results obtained with OBIA (compare fig. 1). However, note that the U-Net was not trained on images of 2016. Therefore, the result illustrates an example of the generalisation capability of the approach (see also appendix fig. A3).

The U-Net segmentation results for the validation year 2016 exhibit a good correspondence to the OBIA results (see fig. 2 and appendix fig. A3 for examples), which we consider as the baseline in this study. In order to obtain well-defined segments, we select a threshold for the pixel-wise probability output of the U-Net. We consider a threshold value of 0.3 which leads to the best agreement between U-Net and OBIA segments with respect to the total degraded area (see fig. 3). Generally, erosion sites with unambiguous boundaries such as shallow landslides (and clear cases of livestock trails) have a better overlap, while erosion sites with more diffuse boundaries (especially sheet erosion and management effects) show slight mismatches compared to the baseline. Quantitatively, we obtain a precision score of 73% and a recall score of 84% (areas of non-/overlapping segments). Note that these scores mainly highlight the difference between the U-Net segmentation with respect to the OBIA segmentation baseline and that both methods might capture valid erosion sites that the other misses. For instance, segments contributing to the 27% false positives could be correctly predicted by the U-Net as it is known that OBIA tends to give a conservative estimate of degraded soil [19].

Ultimately, our goal is to evaluate the total degraded area and study the temporal trend and relative increase in degraded area. To this end, we perform a linear regression to obtain the linear temporal trend in the validation section of our study site over the time period from 2000 to 2016. As fig. 3 (right) illustrates, both the total degraded area as well as the linear trend as predicted by the U-Net lead to similar results as obtained with OBIA for the full probabilistic output of the U-Net as well as a threshold of 0.3. We obtain qualitatively similar results for the individual erosion classes (not shown). Choosing a different probability threshold over- or underestimates degraded area with respect to the OBIA baseline (see fig. 3, left plot). Nevertheless, the relative increase in total degrade area from 2000 to 2016 is less dependent on the threshold choice (see fig. 4), leading to a relative increase of degraded soil of 201% and 167% for the U-Net (0.3 threshold) and OBIA, respectively.

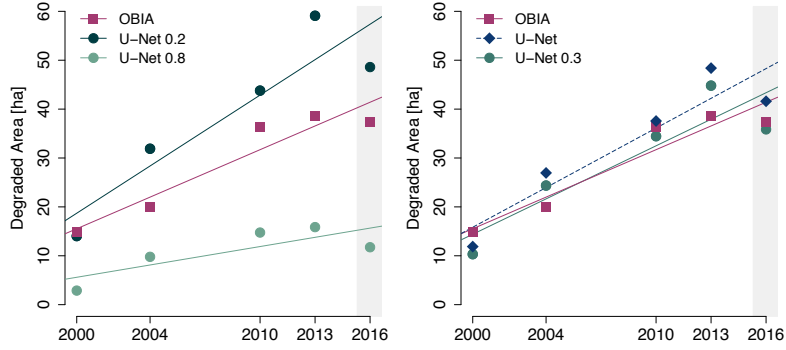


Figure 3: Linear trend of the total degraded area in the validation section as obtained with the OBIA and the U-Net approach. Left: Results for a range of different threshold value are displayed. Right: Results for the suitable threshold value 0.3 (hard segmentation) and the full probabilistic output (without a threshold) are given. Qualitatively, both methods provided similar results with respect to the total degraded soil and linear temporal trend of increase in degraded soil. The shaded column for 2016 indicates that year 2016 was not used for training the U-Net. Note that the OBIA approach requires to be trained on each aerial image of the respective year.

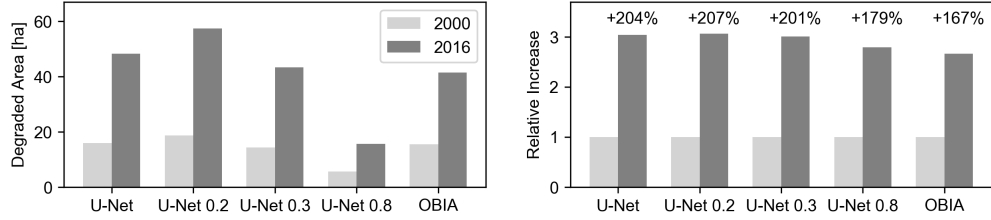


Figure 4: Comparison of total degraded area in years 2000 and 2016 for the OBIA baseline and the U-Net approach with different thresholds. In all approaches, an increase of degraded area in the validation section is observed with threshold-specific differences in the total extent (left panel). However, the relative increase in degraded area (right panel) shows that assessing the trend of soil degradation is less dependent on the choice of threshold.

Apart from good agreement with the OBIA baseline, these results illustrate both the temporal as well as spatial generalisation capability of the U-Net approach, as no image samples of the year 2016 were used and the evaluation was performed on the (held-out) validation section. Crucially, while the OBIA approach in our study requires four to five days of work per aerial image to achieve good segmentation results, the training of a U-Net on a recent GPU (Nvidia Titan X) takes approximately 6.5 hours and prediction takes about 12 minutes for a full aerial image of our case study region.

## 4 Conclusion

In conclusion, by employing classical approaches, a holistic mapping of soil degradation sites in Swiss Alpine grasslands is infeasible due to a high demand on manual adjustments and time requirement. As we show in this study, a properly trained U-Net allows to significantly increase segmentation of aerial images while maintaining outstanding segmentation results on par with standard methods. With this approach, a holistic assessment of the temporal and spatial changes of soil erosion sites in Swiss Alpine grasslands becomes possible. Furthermore, it was shown that the total extent of the considered soil erosion types has increased in the case study region over the considered 16-year period. In addition, the proposed U-Net approach allows including further data sources such as precipitation data or thematic maps on roads, rivers, building footprints. For practitioners an incorporation into geographic information system software like ArcGIS is easily possible and, in fact, already pursued.<sup>3</sup>

<sup>3</sup><https://github.com/Esri/raster-deep-learning>

## Acknowledgements

An extended version of the presented work is currently under review in *Remote Sensing*. The authors would like to thank the Swiss National Science Foundation for supporting the research. This research was funded by Swiss National Science Foundation with the grant number 407540 167333 as part of the Swiss National Research Programme NRP 75 "Big Data". Calculations were performed at sciCORE (<http://scicore.unibas.ch/>) scientific computing core facility at University of Basel. We also want to acknowledge Swisstopo and MeteoSwiss for providing the datasets we used. The authors declare no conflict of interest.

## References

- [1] C. Appenzeller, I. Bey, M. Croci Maspoli, J. Fuhrer, R. Knutti, C. Kull, and C. Schär. Swiss climate change scenarios ch2011. Technical report, ETH Zurich, 2011.
- [2] T. Blaschke. Object based image analysis for remote sensing. *ISPRS journal of photogrammetry and remote sensing*, 65(1):2–16, 2010.
- [3] H. Dong, G. Yang, F. Liu, Y. Mo, and Y. Guo. Automatic brain tumor detection and segmentation using u-net based fully convolutional networks. In *annual conference on medical image understanding and analysis*, pages 506–517. Springer, 2017.
- [4] T. Falk, D. Mai, R. Bensch, Ö. Çiçek, A. Abdulkadir, Y. Marrakchi, A. Böhm, J. Deubner, Z. Jäckel, K. Seiwald, et al. U-net: deep learning for cell counting, detection, and morphometry. *Nature methods*, 16(1):67, 2019.
- [5] N. Flood, F. Watson, and L. Collett. Using a U-net convolutional neural network to map woody vegetation extent from high resolution satellite imagery across Queensland, Australia. *Int. J. Appl. Earth Obs.*, 82:101897, 2019.
- [6] Z. M. Hamdi, M. Brandmeier, and C. Straub. Forest damage assessment using deep learning on high resolution remote sensing data. *Remote Sens.*, 11:1976, 2019.
- [7] L. Ivanovsky, V. Khryashchev, V. Pavlov, and A. Ostrovskaya. Building detection on aerial images using U-NET neural networks. In *Conference of Open Innovation Association, FRUCT*, pages 116–122, 2019.
- [8] T. Kattenborn, J. Eichel, and F. E. Fassnacht. Convolutional Neural Networks enable efficient, accurate and fine-grained segmentation of plant species and communities from high-resolution UAV imagery. *Sci. Rep.*, 9:17656, 2019.
- [9] D. P. Kingma and J. Ba. Adam: A method for stochastic optimization. *arXiv preprint arXiv:1412.6980*, 2014.
- [10] S. Kohl, B. Romera-Paredes, C. Meyer, J. De Fauw, J. R. Ledsam, K. Maier-Hein, S. A. Eslami, D. J. Rezende, and O. Ronneberger. A probabilistic u-net for segmentation of ambiguous images. In *Advances in Neural Information Processing Systems*, pages 6965–6975, 2018.
- [11] N. Mboga, S. Georganos, T. Grippa, M. Lennert, S. Vanhuysse, and E. Wolff. Fully convolutional networks and geographic object-based image analysis for the classification of vhr imagery. *Remote Sensing*, 11(5):597, 2019.
- [12] K. Meusburger and C. Alewell. Impacts of anthropogenic and environmental factors on the occurrence of shallow landslides in an alpine catchment (urseren valley, switzerland). *Natural Hazards and Earth System Sciences*, 8:509–520, 2008.
- [13] K. Meusburger and C. Alewell. On the influence of temporal change on the validity of landslide susceptibility maps. *Natural Hazards and Earth System Sciences*, 9:1495–1507, 2009.
- [14] O. Ronneberger, P. Fischer, and T. Brox. U-net: Convolutional networks for biomedical image segmentation. In *International Conference on Medical Image Computing and Computer-assisted Intervention*, pages 234–241. Springer, 2015.
- [15] Swisstopo. Swissimage: [https://shop.swisstopo.admin.ch/en/products/images/ortho\\_images/SWISSIMAGE/](https://shop.swisstopo.admin.ch/en/products/images/ortho_images/SWISSIMAGE/).
- [16] Swisstopo. SwissALTI3D: [https://shop.swisstopo.admin.ch/en/products/height\\_models/alti3D/](https://shop.swisstopo.admin.ch/en/products/height_models/alti3D/).

- [17] Y. Xu, L. Wu, Z. Xie, and Z. Chen. Building extraction in very high resolution remote sensing imagery using deep learning and guided filters. *Remote Sens.*, 10:144, 2018.
- [18] Y. Yi, Z. Zhang, W. Zhang, C. Zhang, W. Li, and T. Zhao. Semantic segmentation of urban buildings from VHR remote sensing imagery using a deep convolutional neural network. *Remote Sens.*, 11:1774, 2019.
- [19] L. Zweifel, K. Meusburger, and C. Alewell. Spatio-temporal pattern of soil degradation in a swiss alpine grassland catchment. *Remote Sensing of Environment*, 235:111441, 2019.

---

# Segmentation of Soil Degradation Sites in Swiss Alpine Grasslands with Deep Learning

---

## 1 Appendix

### 1.1 Neural Network Architecture

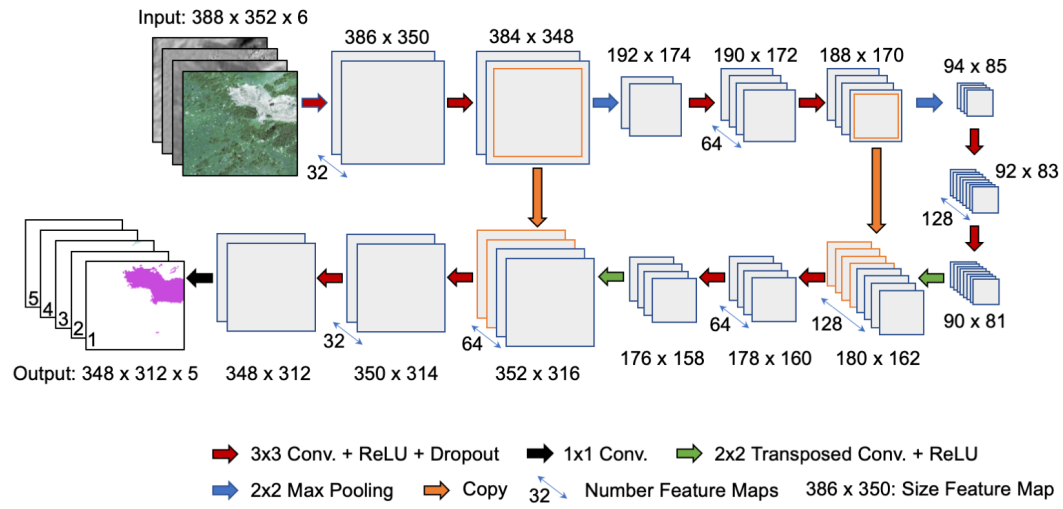


Figure A1: The employed U-Net architecture. The input consists of the input RGB image (three channels) and the DTM derivative maps for the aspect, curvature, and slope (one channel each). The resulting output provides a segmentation map for each considered class: Shallow Landslides (indicated by 1 in the output), Livestock Trails (2), Sheet Erosion (3), Management Effects (4), and a class for non-assignable pixels (5).

## 1.2 Exemplary Training Samples

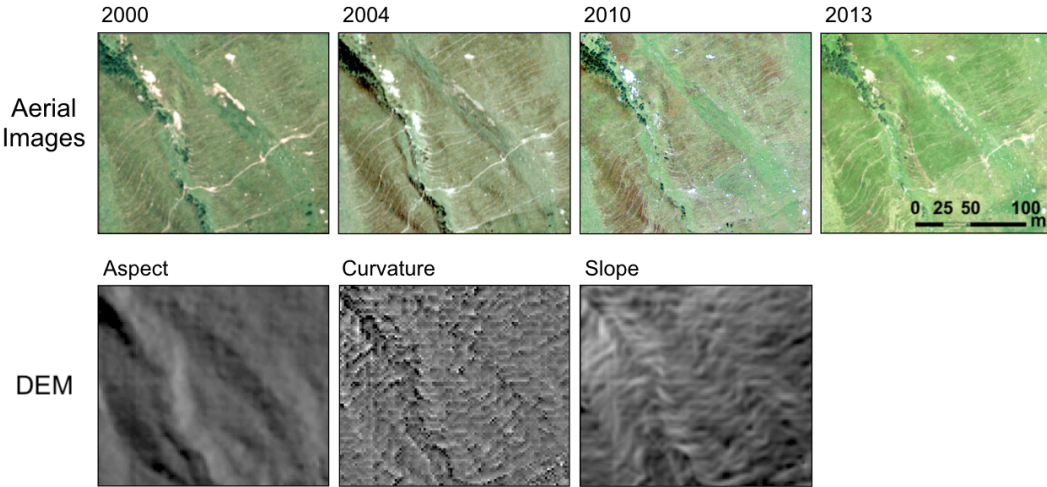


Figure A2: Example of input RGB images for training for the years 2000, 2004, 2010, and 2013 with a size of 194 m × 176 m (corresponding to 388 × 352 pixels at 0.5 m resolution). The images show examples of the same area with eroded soil on grassland slopes (shallow landslides, livestock trails). Below, the corresponding aspect, curvature, and slope maps are displayed. For all years the same DEM information is used.

## 1.3 Segmentation Results on a Validation Section

See fig. A3 below.

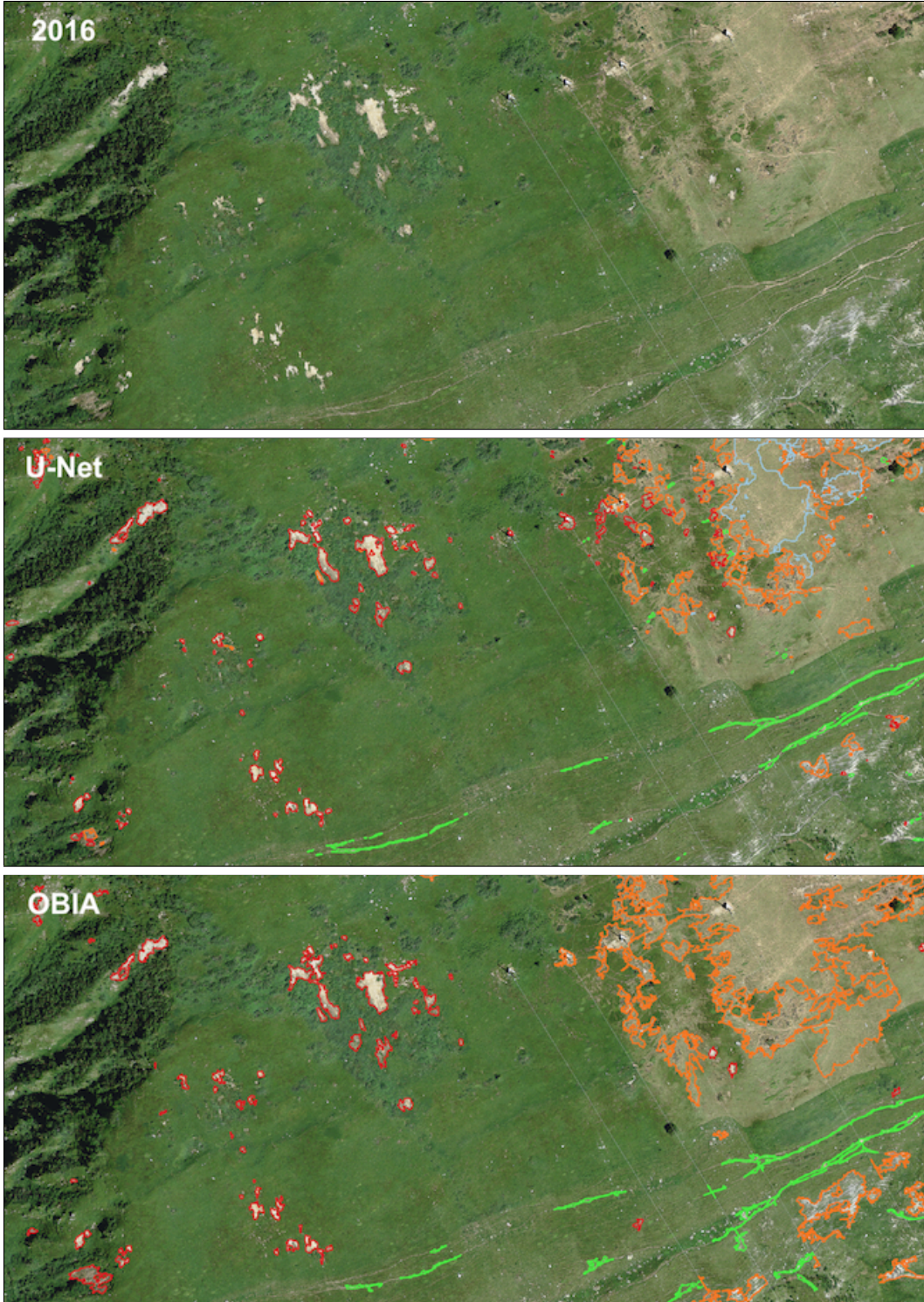


Figure A3: Exemplary segmentation results for a validation section of the case study region in the Swiss Alps. The first panel displays the section of about  $240 \text{ m} \times 500 \text{ m}$  (aerial image from 2016). The middle panel shows the results of the U-Net prediction (threshold of 0.3), while the bottom panel gives the results for the semi-automatic OBIA method. Note that the U-Net was not trained on images of 2016 and the validation section was not included in training with images from previous years. Thus, the result provides an example of the generalisation capability to previously unknown data. In contrast, the OBIA method requires to be trained on the image of 2016 to perform well. Still, the results show great correspondence. As described in the main text, the erosion classes are: **Shallow Landslides**, **Livestock Trails**, **Management Effects**, and **Sheet Erosion**.